ANCS – INCDIE ICPE-CA Exploratory Workshop
ADVANCED MATERIALS FOR ALTERNATIVE ENERGY TECHNOLOGIES:
HYDROGEN BASED ENERGY
Bucharest ROMANIA September 17-19, 2008.

Recent Developments in Hydrogen Materials Modeling

N. Plugaru

Dpto. Ciencia y Tecnologia de Materiales y Fluidos, Centro Politecnico Superior (CPS),
Universidad de Zaragoza, c/ Maria de Luna 3, 50018 Zaragoza, Spain.
and
National Institute of Materials Physics, P.O. Box MG-07, Bucharest-Magurele 77125 Romania.

Contents

1. Motivation

Need of high capacity solid-state storage of hydrogen for
Fuel cells, Automotive and Electrical utility applications

On a weight basis: 120 MJ/kg for hydrogen versus 44 MJ/kg for gasoline.
On a volume basis: 8 MJ/liter for liquid hydrogen versus 32 MJ/liter for gasoline.

Critical issue: to develop proper storage systems that operate at ambient conditions with enough gravimetric capacity and satisfactory H_2 release rates

Hydrogen can be stored in a variety of ways:

- Compressed Gas and Cryogenic Liquid Storage.

- Materials-based Hydrogen Storage on surfaces (by adsorption) or within solids (by absorption).

- Chemical hydrogen storage: through the reaction of H-containing materials with water (or other compounds such as alcohols). It is also possible to store hydrogen in the chemical structures of liquids and solids.

Hydrogen storage in solids may make it possible:

- To store larger quantities of hydrogen in smaller volumes at low pressure and at temperatures close to RT.

- It is possible to achieve volumetric storage densities greater than liquid hydrogen.

Materials for H_2 Storage

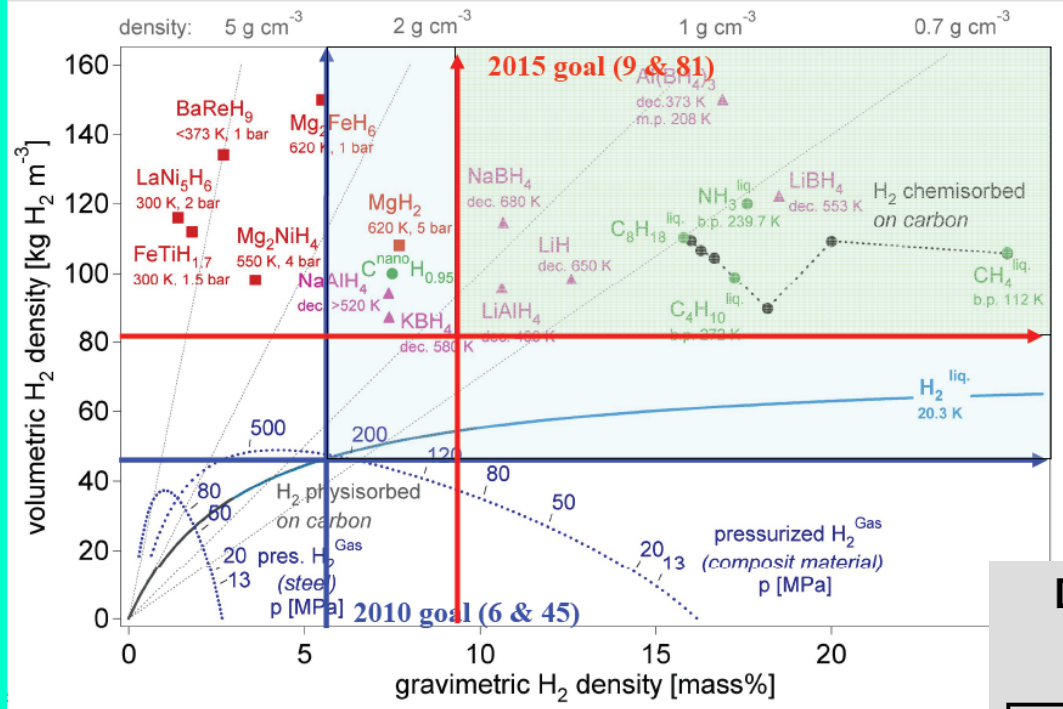

Ref: A. Züttel, "Materials for hydrogen storage", materials today, Septemper (2003), pp. 18-27

Hydrogen storage in solid state:

- Metal hydrides, Alanates

- Chemical hydrides

- Carbon-based materials, Nanostructures (C Nanotubes, Fullerenes, C Nanorods, etc)

- Others (metallo-organic compounds, clathrates, amides, etc.)

DOE (EERE) Hydrogen Storage Challenge

FreedomCAR On-board storage for FC vehicles
Call for "virtual centers" and advanced concepts

Volumetric Density		
year	2010	2015
KWh/liter	1.5	2.7
MJ/liter	5.4	9.7
gm/liter	45	81

Gravimetric Density		
year	2010	2015
KWh/kg	2	3
MJ/kg	7.2	10.8
gm/kg	60	90

Operational temperature: -20 < °C < 80

Material with 9 wt% H_2 that releases H_2 < 80° C

Source: US DOE - Pacific Northwest National Laboratory
MicroNano Breakthrough Conference, Portland, OR, July 27 2004

Hydrogen Storage Challenges

- High capacity
- Decrease in the Weight and Volume of hydrogen storage systems
- Energy efficiency (the energy required to get hydrogen in and out)
- Life-cycle energy efficiency (for chemical hydride storage in which the by-product is regenerated off-board.
- Durability: lifetime of 1500 cycles ?
- Acceptable refueling times

Also, Safety issues, Cost. Codes & Standards
For automotive applications: H storage capacity > 6.5 wt.% (US DOE)

1. Motivation for ***ab initio*** **modeling**

- Intrinsic scientific and intellectual values.

- Electronic structure methods to become an integral part of industrial research.

- They may be used to create direct economic benefits by

Computational Materials Science from First Principles

DFT exploration of the thermodynamic and kinetic properties of hydride materials provides:

- Insight into the fundamental processes, particularly where experiment can not access (e.g. interfaces, boundary regions)

- Rational guidelines for experimentalists to synthesize improved / new materials with high hydrogen weight capacities and reversible hydrogen absorption in ambient conditions.

2. Materials for reversible hydrogen storage: General framework

Carbon-based nanomaterials:

fullerenes, CNTs, graphene, nanocrystalline / porous graphite

- High thermal and chemical stability => good reversibility
- Large surface area and light mass => high gravimetric storage capacity

==> Significant candidates as hydrogen storage materials

Physical adsorption group: most widely studied materials are nano / porous materials, such as Nanoporous carbon structures and Metal-Organic frameworks.

Pacific Northwest National Lab, US DOE
MicroNano Breakthrough Conference Portland, OR 7/27/04

How does nano science improve the efficiency of hydrogen storage?
Hypothesis: Nanophase H storage materials will have different thermodynamic and kinetic properties compared to bulk hydrogen storage materials.
Control Reactivity (enhanced rate of hydrogen release)
Can we prevent fusion of the nanoparticles as the reaction proceeds?
(Do not want to lose nanoproperties !
Use Mesoporous Scaffolds
Expected correlation between the gravimetric capacity and the specific surface Area of the n /p materials.

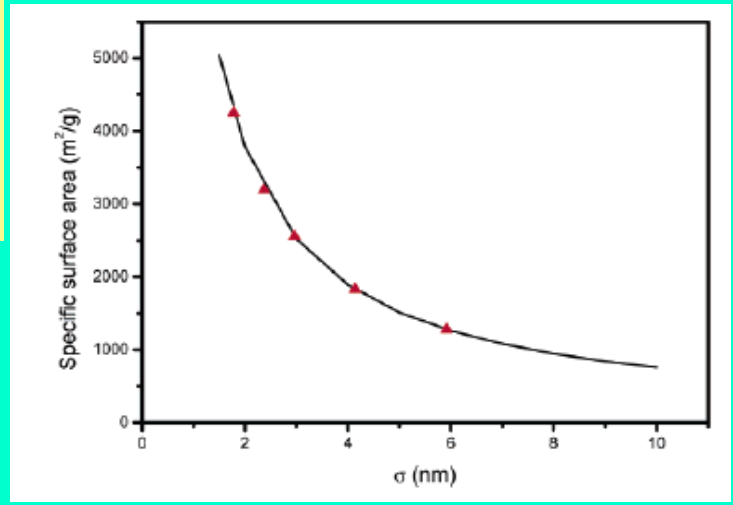

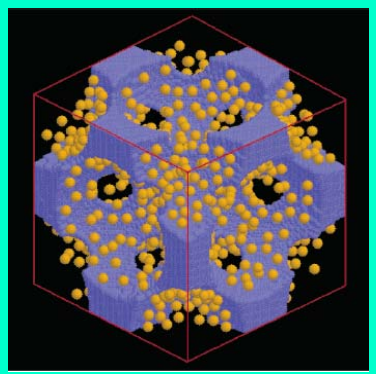

Grand canonical Monte Carlo (GCMC) simulations

Mesoporous carbon

blue network: carbonaceous material,
yellow spheres: hydrogen molecules.

High gravimetric capacity, e.g.of the GCIO materials (5.9 wt % - 5.6 wt % at 30.25 MPa and RT) very close to the target (6.0 wt %) set by the U.S. DOE.
It is closely related to their extraordinarily large specific surface area (4248 - 2554 m^2/g), much larger than that for typical activated carbon and carbon nanotubes.

Economically accessible for mass production
Theoretical predictions not confirmed experimentally (yet)

Cao et al., Nano. Lett. 4(8) (2004) 1489.

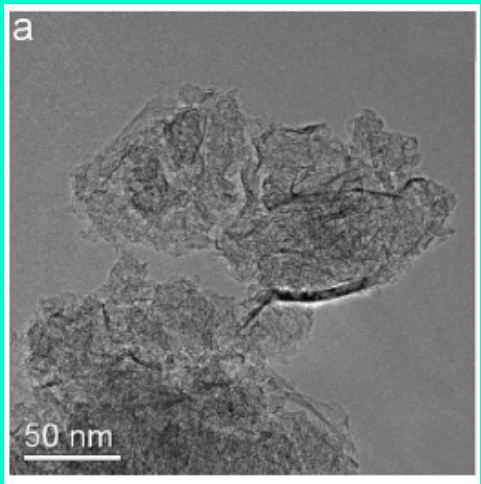

Hydrogen adsorption in ball-milled graphite.
Investigated in the low temperature range from 110 to 35K and at pressures up to 20MPa.
The amount of hydrogen adsorbed at temperatures well below 77K exceeds considerably the expected value from adsorption on graphitic planes.

Proposed mechanisms:
(i) adsorption in trapping states on plane surfaces at and below 110 K;
(ii) adsorption in small micropores with diameter of less than 1 nm at 77K and pressure of 10MPa, and
(iii) multilayer adsorption in mesopores at temperatures from 35 to 40K and pressure of 2MPa.
The effects observed in the low temperature range are reversible

TEM-image of nanostructured powder structure-type "stacking packages" embedded in an amorphous carbon matrix

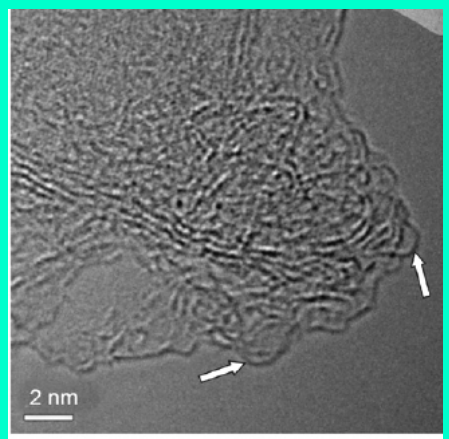

$t_{milling}$=1 h, T_{start}=77 K

TEM-image of microporosity of samples milled at low temperatures.

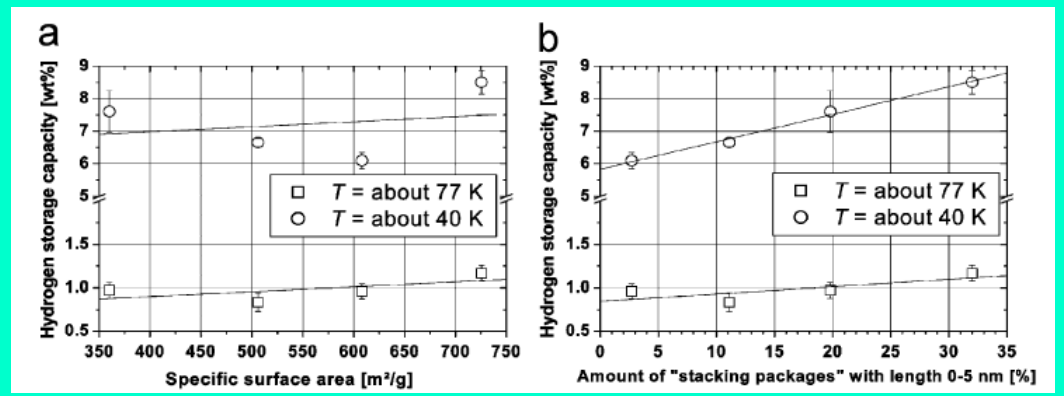

Correlations of the specific surface area (a) and the amount of "stacking packages" (b) to the hydrogen storage capacity.

Hentsche et al., International Journal of Hydrogen Energy 32 (2007) 1530

Carbon Nanostructures:

Single-walled carbon nanotubes (SWNT)- main issue:

- Difficulty in reproducing claimed hydrogen capacities (3-10 wt.% at RT)

- Recent results at NREL (National Renewable Energy Laboratory US DOE)
show that while no hydrogen storage was observed in pure single-walled carbon nanotubes,
- roughly 3 wt.% was measured in metal-doped nanotubes at room temperature, as is shown in the Graph.

- The room temperature gravimetric capacity measured in carbon nanotubes is below the 2010 system target of 6.0 wt.%.
The DOE Hydrogen Program has a go/no-go decision point planned on carbon nanotubes at the end of FY2006
based on a reproducibly demonstrated material hydrogen storage gravimetric capacity of 6 wt.% at room temperature.

Carbon Nanotube Sorption Science External Peer Review of NREL Activities, January 19-23, 2004

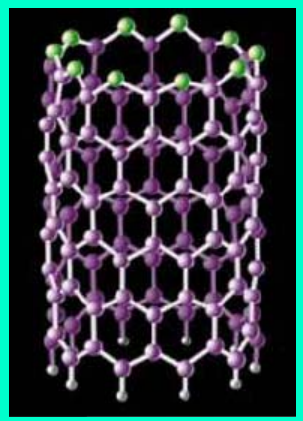

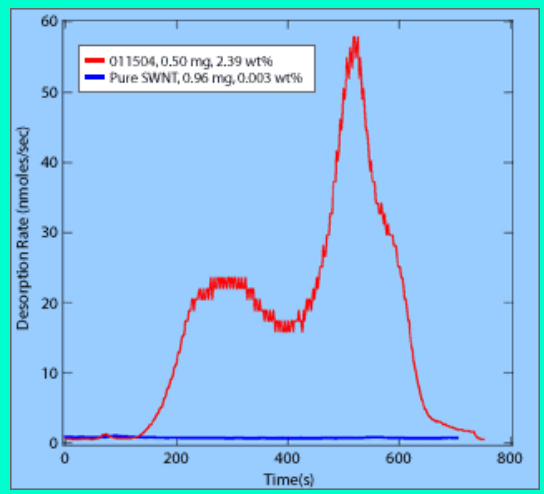

revision of experimental data : pesimistic prediction for H storage in C nanotubes

M. Hirscher et al., J. Alloys and Compounds **356–357** (2003) 433

Hydrogen Storage in Microporous Metal-Organic Frameworks

Metal-organic framework-5 (MOF-5) of composition $Zn_4O(BDC)_3$ (BDC = 1,4 benzenedicarboxylate) with a cubic three-dimensional extended porous structure adsorbed hydrogen up to 4.5 wt.% (17.2 hydrogen molecules per formula unit) at 78 K and 1.0 wt.% at RT and pressure of 20 bar.

Single-crystal x-ray structures of MOF-5 illustrated for a single cube fragment of their respective cubic three-dimensional extended structure. On each of the corners is a cluster $[OZn_4(CO_2)_6]$ of an oxygen-centered Zn_4 tetrahedron that is bridged by six carboxylates of an organic linker. (Zn, blue polyhedron; O,red spheres; C, black spheres). The large yellow spheres represent the largest sphere that would fit in the cavities assuming spherical atoms with van der Waals radii in the framework. (Hydrogen atoms : omitted.)

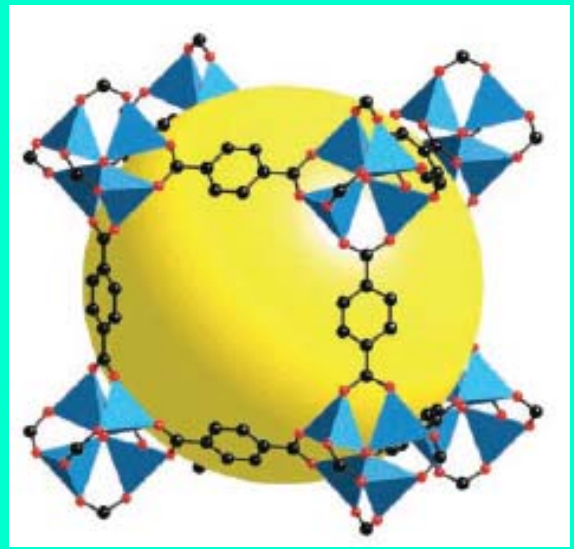

Huge specific surface area: 3000 m^2/g
Pore diameter : 1.3 nm
Max storage at 77K : 4.5% at 1 bar
at RT : 1.0% at 20 bar

N. L. Rosi et al., Science 300 (2003) 1127

Metal Hydrides

Potential for reversible on-board hydrogen storage and release at low temperatures and pressures.
A simple metal hydride such as LaNi5H6 : its gravimetric capacity is too low (~ 1.3 wt. %) and its cost is too high for vehicular applications.

MgH2 theoretical storage capacity of 7.7 wt.%, high reversibility and low cost.

Slow desorption kinetics and desorption T of 573 –714 K, depending on pressure, doping, milling.

AlH3 theoretical storage capacity of 10.1 wt.%.

Low cost and low decomposition T in range T = 333 –473 K.

Volumetric capacity of 0.074 kg H2/l, more than 60% higher than the 2010 volumetric DOE target of 0.045 kg H2/l.

H2 gas pressures > 2.5 GPa are required to rehydride Al back to AlH3.

Klinger et al.: alane might be made at lower T and pressures using nanoparticulate aluminium. 100 nm aluminium particles : equilibrium hydrogenation pressure was 34.2 MPa at 338 K.

Hydrides	Hydrogen gravimetric density (%)	Hydrogen volumetric density (H at.×10^{22} /cm^3)	Density (g/cm^3)
LiH	12.7	5.3	0.8
NaH	4.2	2.3	1.4
MgH_2	7.6	6.7	1.4
$FeTiH_{1.95}$	1.8	6.0	5.47
$TiVCrH_6$	3.6	10-11	5.7
$LaNi_5H_{6.7}$	1.5	7.58	8.25
$LiAlH_4$	10.6	5.74	0.91
TiH_2	4.0	9.0	3.8
VH_2	2.1	10.3	4.5

Maximal gravimetric and volumetric capacities of several metal hydrides.
Note: Li alanate is included for comparison reasons.

Hydrogen storage in complex metal hydrides (M-X-H)
M= e.g. Na, Li, Mg and X= Al or B

Alanates M(AlH4) have the potential for higher gravimetric hydrogen capacities
in the operational window than simple metal hydrides.
Alanates can store and release hydrogen reversibly when catalyzed with titanium dopants

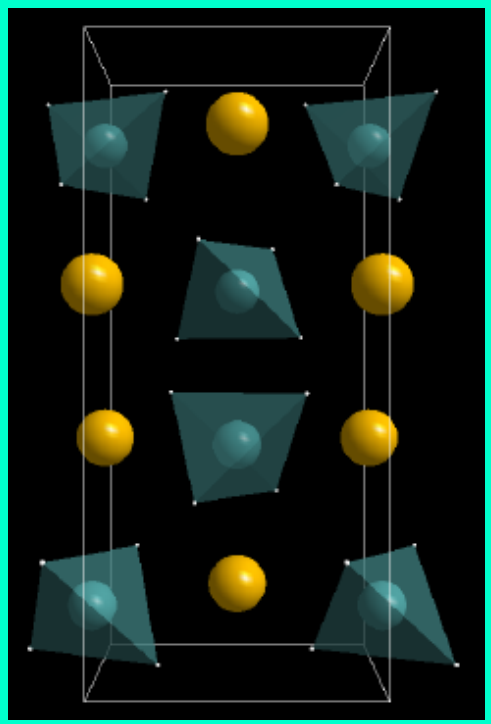

$NaAlH_4$

key alanates

	Accessible (wt.%)	Formation enthalpy (kJ/mol H_2)
$LiAlH_4$	8.0	-55.5
$NaAlH_4$	5.6	-54.9
$KAlH_4$	4.3	-70.0
Li_3AlH_6	5.6	-102.8
Na_3AlH_6	3.0	-69.9
K_3AlH_6	2.0	-78.5
$Mg(AlH_4)_2$	7.0	-21.1
$Ca(AlH_4)_2$	5.9	-59.4

The H absorption in Li and Mg alanates is not reversible !

O.M. Løvvik, Funmat 2006 meeting
(Center for Materials Science and Nanotechnology, University of Oslo)

Borohydrides

Model system is $NaBH_4$
Not reversible under reasonable conditions

- Exhibit good capacity (approx 7.0 wt %)

- Ruthenium catalyst allows easy control, near instantaneous reaction

- Exothermic reaction allows direct coupling with PEM fuel cell

- The higher capacity LiBH4 is also considered.

Amendolaa et al., Int. J. Hydrogen Energy **25** (2000) p. 969

3. Ab initio modeling and predictions

First principles COMPUTATIONAL APPROACHES

Density Functional Theory (DFT)

Weakly correlated electron systems:
DFT - LDA **successful**, most notably through its Car-Parrinello MD implementation.

Major failures: e.g., determination of reaction barriers.

Strongly correlated electron systems (most notably those involving partially filled d- and f- shells),
DFT-LDA methods (as well as their extensions, like GGA) : not successful

(sometimes suffer major failures even in the prediction of ground-state properties)

3. Ab initio modeling and predictions

Objective: Hydrogen sieving and H_2 storage in fullerene intercalated graphite by physisorption

Problem: thermodynamically impossible for H2 to penetrate between the layers of graphite !

Solution: increase the interlayer distance of graphite (3.4 Å) to 6 Å - optimal distance where H_2 could penetrate into the material.

The interlayer distance can be increased by
- **Functionalization** of the sheets (fluorination, doping with Li complexes, oxidation with aquas acid agents)
 ==> interlayer distances from 4.7 to 9 Å
Alternative: **Intercalation of spacer molecules**.

The interaction of H_2 with the carbon nanostructure is strongly influenced by the entropy of the system
=> the interaction free energies have to be calculated.

Computational method: Dispersion Corrected (DC) DFT-based tight-binding (**DFTB**) method (**deMon code**)
Quantum mechanical route to calculate the free energy of the system
The H_2-CIG interaction is described by employing a Lennard-Jones potential.

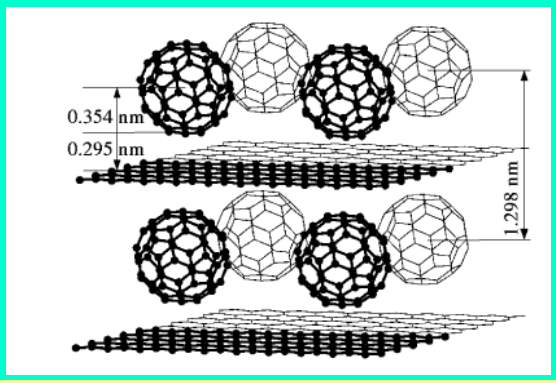

The extended unit cell of C60-intercalated graphite.
The fullerene cages form two-dimensional hexagonal layers.

The interaction potential between H2 and C60-intercalated graphite (H2-CIG).
The figure shows potential energy isosurfaces in a diagonal cut through the unit cell.

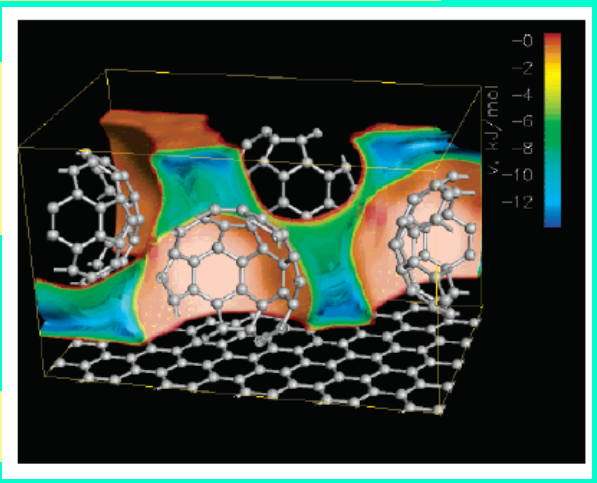

Ref.: Kuc et al., Nano Letters **7** (2007) 1.

- The simulations confirm the CIG structure

- Exp. and simulation closely agree on the geometrical parameters.

-The electronic properties of CIG are similar to those of graphite.

- The shape of the spacers allows a nearly free penetration of H_2.
➔ easy loading and unloading (advantage over metal hydrides and alkali-doped carbon structures.

- No effect on its structural and mechanical properties !

- The spacers double the interaction free energy of the material with H2 in the limit of the low hydrogen gas pressure.

- Bad news: the fullerenes reduce the active volume
(62% of the structure without spacers to 19% in CIG)

- Gravimetric and volumetric storage capacities of H2 in CIG
Close to values for Li-doped carbon systems (low T) see Table.

- The storage capacity : interesting for practical applications at low T and moderate pressures (e.g., at 10 MPa and 200 K).

- **A more promising material** : **reduce the density of C_{60} inside CIG**.

-CIG a useful part of a composite storage system: in situ separation
-of H_2 from other gases (molecular sieving.)

Table 2. Hydrogen Storage Capacities of Selected Materials[a]

material	T (K)	P_{ext} (MPa)	gw (%)	V_c (g/cm^3)
CNT	298−773	0.1	0.4 (0.3/0.7)[b]	0.0032
Li-doped CNT	473−673	0.1	20.0	0.180
Li-doped graphite	473−673	0.1	14.0	0.280
K-doped CNT	<313	0.1	14.0	0.0126
K-doped graphite	<313	0.1	5.0	0.060
FeTi−H	>263	2.5	<2	0.096
NiMg−H	>523	2.5	<4	0.081
cryoadsorption	~77	20	~5	0.020
isooctane/gasoline	>233	0.1	17.3	0.117
CIG	300	10	(3.5)	(0.060)
	250	10	(5.7)	(0.071)
	200	10	(9.1)	(0.120)

[a] The storage temperature (T), external pressure (P_{ext}), gravimetric density (gw), and volumetric density (V_c) are compared. Experimental values are taken from ref 28, while those calculated for this work are given in parentheses. [b] Model calculations of a carbon nanotube with chirality (6,6) and ~7 Å diameter at ambient conditions give gravimetric storage capacities of 0.3% in the interior of a CNT and 0.7% in a bundle.

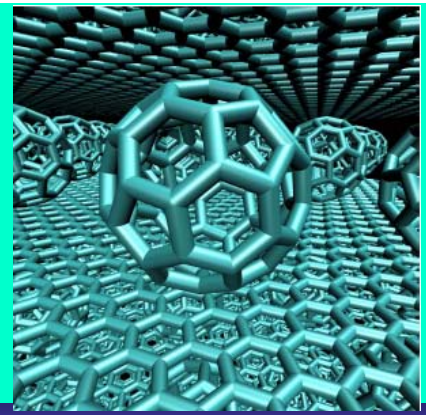

Ref.: Kuc et al., Nano Letters **7** (2007) 1.

Kim et al., Phys. Rev. B**78** (2008) 085408

Optimization of metal dispersion in doped graphitic materials for hydrogen storage

The TM-H binding energy and ratio: promising with respect to the capacity and release temperature.
Problem: strong tendency of TM atoms to cluster !

Solution Noncovalent hydrogen binding on TM atoms dispersed on carbon clusters and graphene.

Mechanism The presence of acceptor-like states in the absorbents is essential for
- increase in TM adsorption strength
- increase in number of H_2 attached to the TM atoms.

Study of sp2-like bonded carbon materials : graphene and coronene molecules.
building blocks of porous structures that can host metals and hydrogen molecules.
Strong Interest in the effect of charge transfer between dopants - TM atoms and H_2

Computational method

LSDA and **GGA** total-energy calculations, **VASP** code.
(projector augmented wave pseudopotentials).

Optimized structures of Ti attached to
(a) pure
(b) B-doped coronene molecule.

Yellow- C, **purple- B**, **blue- Ti**, light blue- Saturating H atoms.

(c) Calculated binding energies of TM = Sc, Ti, V on B- or N-doped coronenes. *n* = number of B or N atoms in a carbon hexagon ring without forming B-B or N-N bonding.

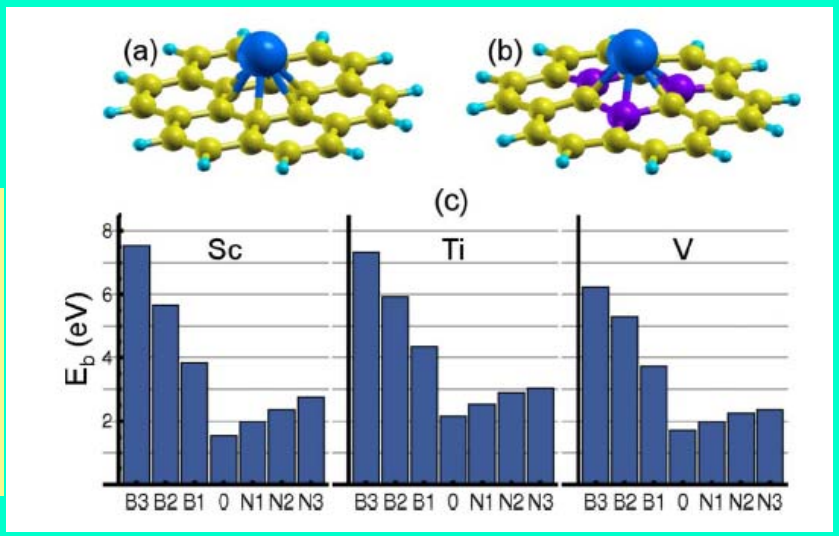

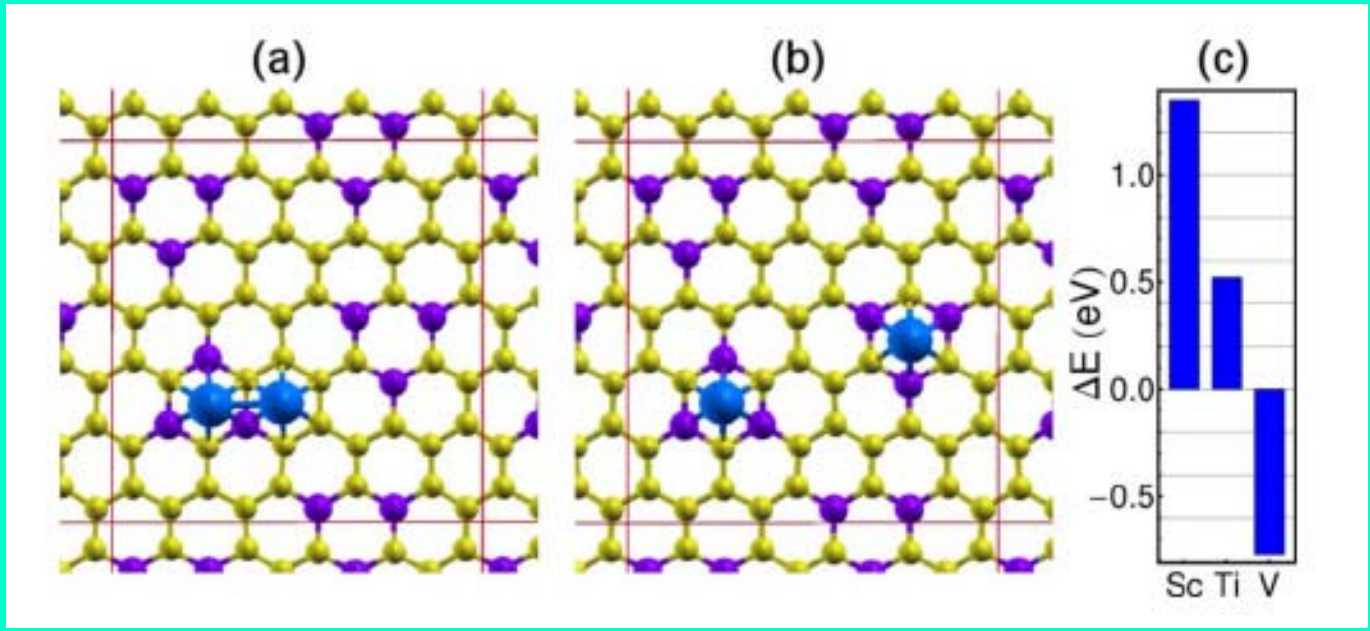

Two TM atoms on B-doped graphene of $C_{48}B_{12}$
(a) TM dimer
(b) separated TM atoms
(c) The energy difference between geometries in (a) and (b) for Sc, Ti, and V. **Configuration (b) has a larger cohesive energy than (a).**

Boron substitutional doping provides acceptor-like states
=> improved doping conditions for hydrogen storage.

Kim et al., Phys. Rev. B**78** (2008) 085408

Chen et al., Phys. Rev. B**77** (2008) 033405.

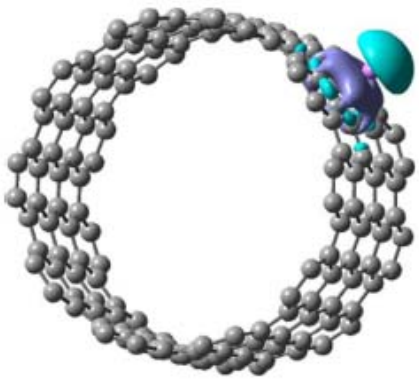

Isosurface of charge density plot for Li coated (10, 10) CNT.
D=*D*(Li–CNT) - *D*(CNT) - *D*(Li)
Blue and purple ::positive and negative charge distributions.

Objective: To increase the H_2 binding energy to CNTs.

Supercell calculations DFT - GGA.
Ionic cores replaced by ultrasoft pseudopotentials - VASP code.
Calculations of H_2 interaction with
pure nanotube
Li-doped nanotube
Li-doped nanotube peapod structures.

Problem: H_2 wt % for pure CNT structures may not exceed 1 wt %.
The binding of H_2 on CNT surface is van der Waals in nature - binding energy range from 20 to 100 meV.

Ti prefers to cluster on CNT surfaces.
Clustering of Li atoms is energetically highly unfavorable

The increase in H_2 binding is due to the direct interaction between Li ion and H_2 molecule.
Charge transfer from
CNT to C_{60} molecule ➔ charge transfer from Li to the CNT ➔ Li deposited on peapod structure more positive

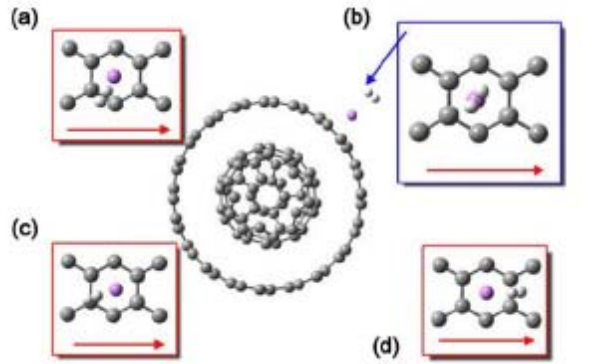

BAD NEWS: 300 meV interaction energy required for RT hydrogen adsorption and desorption process !

TABLE II. Binding energy of Li and Li-nanotube surface distance on nanotube and nanopeapod structures. Also, the binding energy of H_2 molecule and H–Li bond distance on nanotube and nanopeapod structures.

System studied	Distance (Å)	Binding energy
Li on nanotube	1.76	1.64 eV
Li on nanopeapod	1.71	1.76 eV
H_2 on Li coated nanotube	2.10	180 meV
H_2 on Li coated nanopeapod	2.08	217 meV

Lee et al., Phys. Rev. B **77** (2008) 235101.

Room-temperature dissociative hydrogen chemisorption on boron-doped fullerenes

Motivated by the fact that
B-doped fullerenes, $C_{54}B_6$, $C_{59}B$, and $C_{58}B_2$ have been successfully synthesized

First-principles (VASP code) and model calculations for trapping-mediated dissociative chemisorption of the H_2 molecule on $C_{54}B_6$.

Using the Polanyi–Wigner equation with the van't Hoff–Arrhenius law, and also MD simulation, => even if a H_2 molecule is nondissociatively adsorbed on the *B*-doped fullerene initially, it becomes dissociative after approx. 0.5 ps at RT.
(In $C_{54}B_6$ the state of molecular adsorption is about 0.47 eV higher in energy than that of dissociative adsorption.)

Possibility of Hydrogenation of $C_{54}B_6$ without catalysts or additional treatments (such as atomic hydrogen beam, hydrogen plasma, and high temperature) at the standard temperature and pressure (STP).

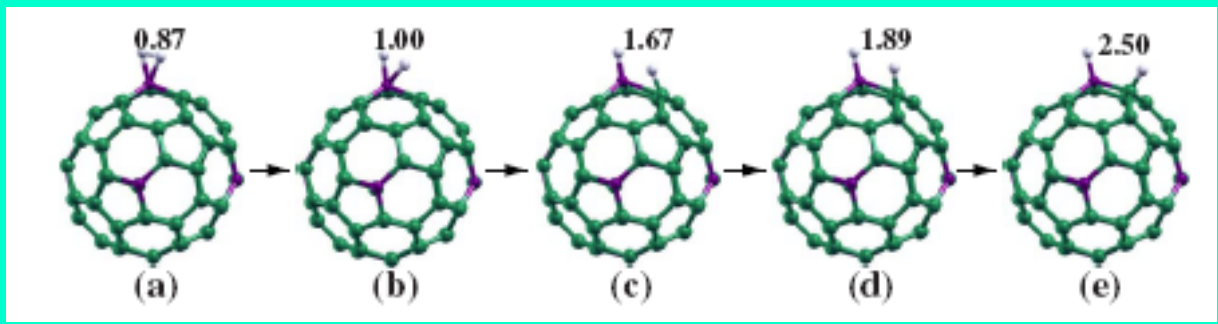

Structures corresponding to the minimum energy pathway for dissociation of the H_2 molecule.

$BaReH_9$ and $BaMnH_9$: Density functional calculations and prediction of $(MnH_9)^{2-}$ salts

$BaReH_9$: family of hydrides based on $(ReH9)^{2-}$ and $(TcH_9)^{2-}$ structural units.

TM atom in a high formal valence state of 7, coordinated by nine H atoms.

Practical interest : the high hydrogen-to-metal ratio = 4.5 in BaReH9.

No Mn based compounds synthesized to date ...

Computational method: LDA - LAPW

Calculation results

- the high coordination in $BaReH_9$ is due to bonding between Re 5d and d-like states formed from combinations of H s orbitals in the H9 cage. [This explains the structure of the material, its short bond lengths and the high band gap (3.58 eV)].
- Similar bonding is found in hypothetical $BaMnH_9$.
- Both compounds have similar cohesive energies.
- BaMnH9 : not a favorable target due to the stability of BaH2 competing phase,
- Suggestion: synthesis of (MnH9)2− salts may be possible

(Note: the chemistry of Mn VII is different than that of Re VII)

(Mg, or Be) (MnH_9) : hydrogen contents >10 wt. % .

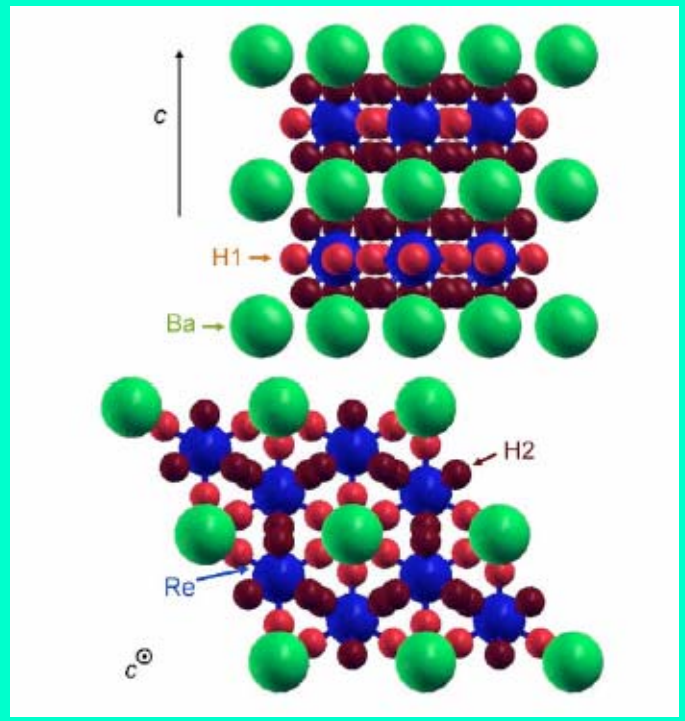

Structure of BaReH9
(top) Ba and ReH9 layers stacked along the *c* axis; (bottom) the hexagonal planes.

Singh et al., Phys. Rev B **75** (2007) 035103.

Hydrogen Storage in Magnesium Clusters: Quantum Chemical Study

Objective: study of cluster size dependency of the (de)sorption enthalpy of MgH_2 versus Mg + H_2.

- Ab initio Hartree-Fock and DFT calculations of the energies of Mg and MgH2 clusters of up to 56 Mg atoms.
- GAMESS-UK program, version 6.0, on the TERAS computer of SARA.

- Magnesium hydride clusters larger than Mg19H38 have a rutile-like geometry, similar to that of bulk β-MgH2.

- For clusters with 56 Mg atoms: calculated desorption energy in agreement with exp. bulk desorption enthalpy (75 kJ/mol [H2])

- Decrease in the cluster size below 19 Mg atoms => decrease in desorption energy
=> lower hydrogen desorption temperature: **A cluster of 0.9 nm would correspond to a desorption temperature of 473 K**.

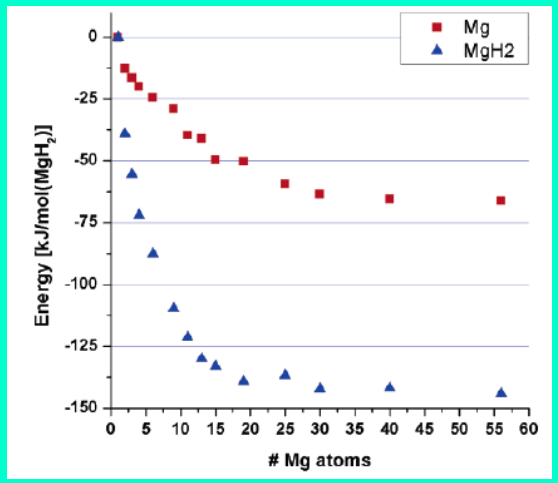

DFT calculations (B97 functional). Energies are scaled to Mg or MgH2 cluster and normalized per Mg atom.

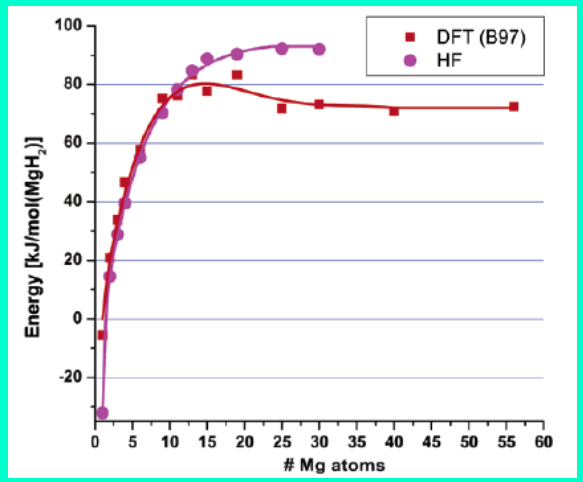

Calculated desorption energies for MgH2 clusters. The energies are normalized per released H2 mole.

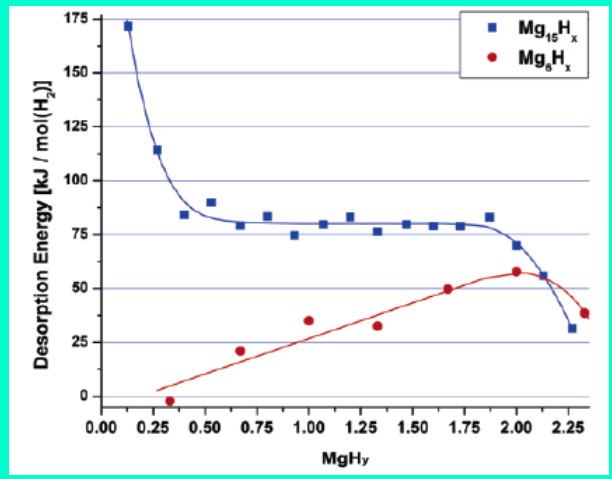

Stepwise dehydrogenation of clusters with 6 and 15 Mg atoms, DFT (B97) calculations. The relative desorption energies normalized per released H2 mole.

Wagemans et al., *J. Am. Chem. Soc.***127** (2005) 16675

Role of charged defects and impurities in kinetics of hydrogen storage materials

First-principles calculations of the creation of hydrogen-related point defects in NaAlH4 and their diffusion through the material.

DFT-GGA and the projector augmented wave method, **VASP** code

Calculations of migration barriers : the nudged elastic band (NEB) method.

- Hydrogen-related point defects play a decisive role in (de)hydrogenation reactions in NaAlH4.

- Charged defects => their formation energy and concentration strongly affected by electrically active extrinsic impurities in the material.

- Hydrogen-related point defects also induce significant rearrangements of the local lattice of the host,

- The relevant point defects and impurities introduce defect levels deep in the band gap => the Fermi-level positions far from the band edges
Defects with the lowest formation energy have the highest concentrations

- the concepts are general - may apply to other hydrogen storage materials.
Suggestion: improved preparation methods for complex hydrides through enhanced control of the addition of small concentrations of impurities.

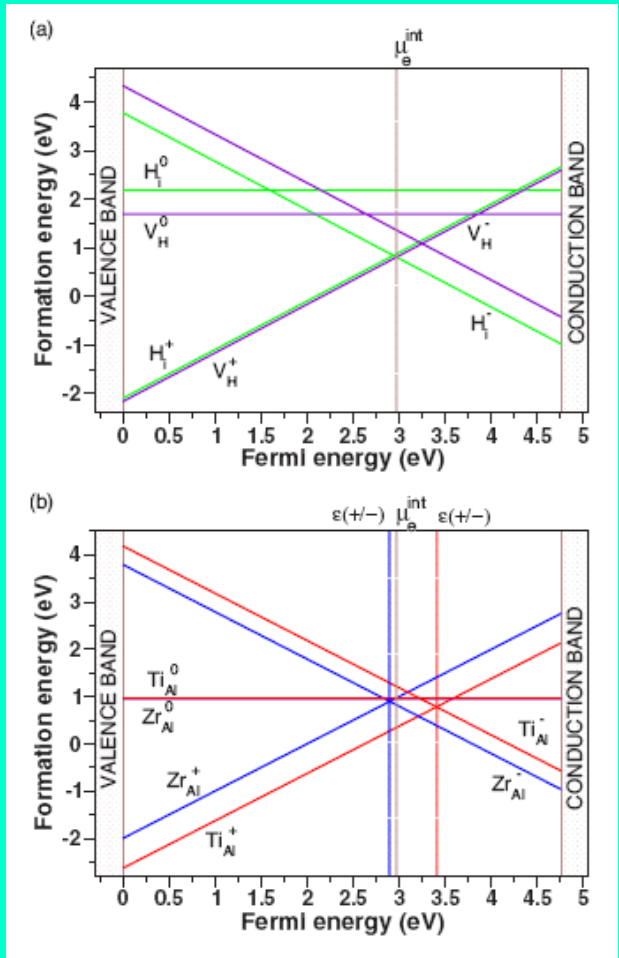

Calculated formation energies of relevant defects and impurities in NaAlH4 as a function of Fermi level. The vertical lines denote the Fermi-level position determined by charge neutrality.
(a) Hydrogen-related defects. Equilibrium with H2 molecules at *T*=0 is assumed.
(b) Ti-related (red) and Zr-related (blue) defects. For Ti and Zr, the chemical potentials were fixed to the energy of the bulk metals and Al-rich conditions were assumed.

Peles and Van de Walle, Phys. Rev. B **76** (2007) 214101

4. Concluding remarks

- **"Engineered"** Carbon-based nanostructured / porous materials and Metal-Organic frameworks show **promising characteristics** for hydrogen storage devices.

- The **computational approach** may provide useful **structural, electronic and energetic** information of the material.

- The role of ***ab initio*** **methods** in materials modeling will **increase** as the materials **complexity increases**.

- **Computational experiment** is a relatively **non expensive approach to guide technological research.**

Outlook

Hydrogen will be a future energy carrier.

5. References

D. Cao, P. Feng and J. Wu, Nano Letters **4** (2004) 1489.
L. Chen, Y. Zhang, N. Koratkar, P. Jena and S. K. Nayak, Phys. Rev. **B77** (2008) 033405.
M. Hentsche, H. Hermann, D. Lindackers, G. Seifert, International Journal of Hydrogen Energy **32** (2007) 1530.
M. Hirscher, M. Becher, M. Haluska, F. von Zeppelin, X. Chen, U. Dettlaff-Weglikowska, S. Roth,
J. Alloys and Compounds **356–357** (2003) 433.
G. Kim, S. H. Jhi, N. Park, S. G. Louie and M. L. Cohen, Phys. Rev. **B78** (2008) 085408.
A. Kuc, L. Zhechkov, S. Patchkovskii, G. Seifert and T. Heine, Nano Letters **7** (2007) 1.
H. Lee, J. Li, G. Zhou, W. Duan, G. Kim and J. Ihm, Phys. Rev. **B77** (2008) 235101.
O.M. Løvvik, Funmat 2006 meeting (Center for Materials Science and Nanotechnology, University of Oslo).
A. Peles and C. G. Van de Walle, Phys. Rev. **B76** (2007) 214101.
N. L. Rosi, J. Eckert, M. Eddaoudi, D.T. Vodak, J. Kim, M. O'Keeffe and O. M. Yaghi, Science **300** (2003) 1127.
G. Seifert , Invited lecture, CARBON07, Seattle, July 2007.
D. J. Singh, M. Gupta and R. Gupta, Phys. Rev **B75** (2007) 035103.
R. W. P. Wagemans, J. H. van Lenthe, P. E. de Jongh, A. J. van Dillen and K. P. de Jong,
J. Am. Chem. Soc. **127** (2005) 16675.
http://www.eere.energy.gov/hydrogenandfuelcells/storage/
http://www.whitehouse.gov/omb/budget/

Acknowledgment

The collaboration with

Prof. M. Artigas (Universidad de Zaragoza)

is gratefully acknowledged.

Thank you for your attention !

deMon code : density of Montréal

- uses the linear combination of Gaussian-type orbital (LCGTO) approach for the self-consistent solution of the Kohn-Sham (KS) DFT equations.

Some of the features of the deMon package are:

- Variational fitting of the Coulomb potential
- Geometry optimization and transition state search
- Molecular dynamic simulations (MD)
- Time-dependent DFT (TD-DFT)
- Calculation of properties like polarizabilities, hyperpolarizabilities, NMR, IR and Raman spectra and
- intensities, thermodynamic data
- Parallelized code (MPI)

VASP code

VAMP/VASP : ab-initio quantum-mechanical molecular dynamics (MD)
using pseudopotentials and a plane wave basis set.

The approach implemented in VAMP/VASP is based on a finite-temperature
local-density approximation (with the free energy as variational quantity) and
an exact evaluation of the instantaneous electronic ground state at each MD-step
using efficient matrix diagonalization schemes and an efficient Pulay mixing.

These techniques avoid all problems occurring in the original Car-Parrinello method
which is based on the simultaneous integration of electronic and ionic equations
of motion.

The interaction between ions and electrons is described using ultrasoft Vanderbilt
pseudopotentials (US-PP) or the projector augmented wave method (PAW).

Both techniques allow a considerable reduction of the necessary number of plane-waves
per atom for transition metals and first row elements.
Forces and stress can be easily calculated with VAMP/VASP and used to relax atoms into
their instantaneous groundstate.

Car-Parrinello Molecular dynamics (PCMD) code

Plane wave/pseudopotential implementation of Density Functional Theory, particularly designed for ab-initio molecular dynamics.

The main characteristics are:

- works with norm conserving or ultrasoft pseudopotentials;

- LDA, LSD and the most popular gradient correction schemes;

- free energy density functional implementation;

- isolated systems and system with periodic boundary conditions;

- k-points; molecular and crystal symmetry;

- wavefunction optimization: direct minimization and diagonalization; geometry optimization: local optimization and simulated annealing;

- molecular dynamics: constant energy, constant temperature and constant pressure; path integral MD; response functions; excited states; many electronic properties.